

Sphingomyelin and sphingomyelin synthase (SMS) in the malignant transformation of glioma cells and in 2-hydroxyoleic acid therapy

Gwendolyn Barceló-Coblijn^{a,1}, Maria Laura Martin^{a,1}, Rodrigo F. M. de Almeida^b, Maria Antònia Noguera-Salvà^a, Amaia Marcilla-Etxenike^a, Francisca Guardiola-Serrano^a, Anja Lüth^c, Burhard Kleuser^c, John E. Halver^{d,2}, and Pablo V. Escriba^{a,1,2}

^aLaboratory of Molecular Cell Biomedicine, Department of Biology, University of the Balearic Islands, Carretera de Valldemossa Km 7.5, E-07122 Palma, Balearic Islands, Spain; ^bCentro de Química e Bioquímica, Faculdade de Ciências da Universidade de Lisboa, Campo Grande, Edifício C8, 1749-016 Lisbon, Portugal; ^cUniversity of Potsdam, Institute of Nutritional Science, Department of Nutritional Toxicology, Arthur-Scheunert-Allee 114-116, 14558 Nuthetal, OT Bergholz-Rehbrücke, Germany; and ^dSchool of Aquatic and Fishery Sciences, University of Washington, Seattle, WA 98195

Contributed by John E. Halver, September 28, 2011 (sent for review August 23, 2011)

The mechanism of action of 2-hydroxyoleic acid (2OHOA), a potent antitumor compound, has not yet been fully elucidated. Here, we show that human cancer cells have markedly lower levels of sphingomyelin (SM) than nontumor (MRC-5) cells. In this context, 2OHOA treatment strongly augments SM mass (4.6-fold), restoring the levels found in MRC-5 cells, while a loss of phosphatidylethanolamine and phosphatidylcholine is observed (57 and 30%, respectively). The increased SM mass was due to a rapid and highly specific activation of SM synthases (SMS). This effect appeared to be specific against cancer cells as it did not affect nontumor MRC-5 cells. Therefore, low SM levels are associated with the tumorigenic transformation that produces cancer cells. SM accumulation occurred at the plasma membrane and caused an increase in membrane global order and lipid raft packing in model membranes. These modifications would account for the observed alteration by 2OHOA in the localization of proteins involved in cell apoptosis (Fas receptor) or differentiation (Ras). Importantly, SMS inhibition by D609 diminished 2OHOA effect on cell cycle. Therefore, we propose that the regulation of SMS activity in tumor cells is a critical upstream event in 2OHOA antitumor mechanism, which also explains its specificity for cancer cells, its potency, and the lack of undesired side effects. Finally, the specific activation of SMS explains the ability of this compound to trigger cell cycle arrest, cell differentiation, and autophagy or apoptosis in cancer cells.

anticancer | membrane-lipid therapy | lung cancer | membrane lipids

The potent antitumor compound 2-hydroxyoleic acid (2OHOA) (Minerval®) acts against cancer by inducing cell cycle arrest (1–3), followed by apoptosis in human leukemia cells (4) or differentiation and autophagy in the case of human glioma cells. Despite the potency of 2OHOA against cancer, it is a safe nontoxic compound with IC₅₀ values in nontumor cells 30- to 150-fold greater than in tumor cells (4). The high efficacy and low toxicity of this fatty acid produce a wide therapeutic window that can only be the consequence of a highly specific mechanism of action, the molecular bases of which have, in part, been elucidated here.

The 2OHOA compound was designed rationally to reproduce the antitumor effect of anthracyclines via interactions with the plasma membrane and the ensuing modifications in cell signaling (5), without unspecific interactions with other cell targets. It is known that 2OHOA binds to membranes and modifies the biophysical properties of the lipid bilayer, the first target encountered by this synthetic lipid (6). Nevertheless, the regulatory effects of 2OHOA on the composition of cancer cell membranes have yet to be described. In fact, 2OHOA induces changes in the localization and activity of membrane proteins involved in cancer cell proliferation, differentiation and survival, such as the Fas receptor (4), PKC (3), as well as cyclins, cyclin-dependent kinases (CDKs), caspases, E2F-1 and dihydrofolate reductase (DHFR)

(1, 2). Interestingly, a similar mechanism is described for edelfosine, a synthetic ether lipid with a high apoptotic activity that also induces reorganization of membrane rafts, FasR capping, and cell apoptosis (7).

Sphingomyelin (SM) is a key component of the plasma membrane that interacts with cholesterol and glycerophospholipids, thereby participating in the formation and maintenance of lipid microdomains. Lipid rafts are important signaling platforms whose structure is sensitive to membrane lipid composition (8), as are the proteins that interact with these and other membrane microdomains (9, 10). Therefore, modifications in SM content affect lipid raft associated signaling pathways. SM is synthesized by SM synthase (SMS) isozymes that catalyze the transfer of a phosphocholine moiety to the primary hydroxyl group of ceramide to form SM and 1,2-diacylglycerol (1,2-DAG) (11). Thus, SMS lies at the crossroads between the two main groups of membrane lipids (glycerophospholipids and sphingolipids) and between two key signaling molecules in cell cycle regulation (ceramide and 1,2-DAG) (12, 13). Consequently, regulating SMS activity will have important consequences on the cell physiology.

In this study, we describe how 2OHOA regulates SMS activity in cancer cell membranes but not in those of nontumor cells, and the concomitant changes in the levels of SM and other lipids. We demonstrate that exposing tumor cells to 2OHOA promotes a robust increase in SM mass through the rapid and specific activation of SMS isozymes. In addition, studies in model membranes showed that these marked changes in lipid composition caused by 2OHOA affect the biophysical properties of membrane microdomains. The rapid activation of SMS by 2OHOA and the subsequent accumulation of SM can at least in part explain the ability of this compound to trigger cell cycle arrest, cell differentiation, and autophagy or apoptosis in cancer cells. Importantly, this report shows that 2OHOA has differential and specific effects against cancer cells.

Results

We assessed the capacity of 2OHOA to diminish the viability of human U118 glioma cells using the XTT method (2,3-bis[2-methoxy-4-nitro-5-sulfophenyl]-2H-tetrazolium-5-carboxyanilide inner salt) and evaluating its effect on DHFR levels, a protein

Author contributions: G.B.-C., J.E.H., and P.V.E. designed research; G.B.-C., M.L.M., R.F.M.d.A., M.A.N.-S., A.M.-E., F.G.-S., and P.V.E. performed research; G.B.-C., M.L.M., A.L., B.K., J.E.H., and P.V.E. analyzed data; and G.B.-C., J.E.H., and P.V.E. wrote the paper.

The authors declare no conflict of interest.

Freely available online through the PNAS open access option.

¹G.B.-C. and M.L.M. contributed equally to this work.

²To whom correspondence should be addressed. E-mail: halver@u.washington.edu or pablo.escriba@uib.es.

This article contains supporting information online at www.pnas.org/lookup/suppl/doi:10.1073/pnas.1115484108/-DCSupplemental.

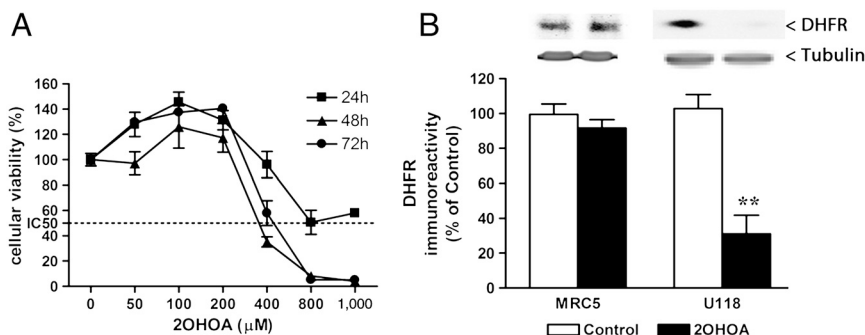


Fig. 1. The 2OHOA compound inhibits cell viability and downregulates DHFR levels in U118 cells. (A) Cell viability assessed by XTT assay. (B) DHFR protein levels in MRC-5 and U118 cells after treatment with 2OHOA (48 h, 200 μ M) as determined by immunoblotting (a representative immunoblot is also shown). Values represent the mean \pm SEM; $n = 3$; **, $P < 0.01$.

downregulated in other cancer cells treated with 2OHOA (1). In this context, 2OHOA reduced the viability of human U118 glioma cells in a concentration-dependent manner (Fig. 1A). 2OHOA (200 μ M, 48 h) also induced a marked and significant decrease in the DHFR protein levels (69.7%) in U118 cells, whereas it had no such effect in the nontumor human lung fibroblast (MRC-5) cells (Fig. 1B). These results extend previous studies, showing that 2OHOA has a distinct effect on DHFR in tumor and nontumor cells (1, 3, 4).

Then, we investigated the impact of 2OHOA treatment (200 μ M, 72 h) on U118 cells lipid mass. Thus, treatment with 2OHOA induced a marked and significant increase in SM mass (4.6-fold) (Table 1 and Fig. 2A) and a decrease in phosphatidylethanolamine (PE) and phosphatidylcholine (PC) mass (57 and 30%, respectively). In addition, phosphatidylserine (PS) mass also decreased 43%, whereas phosphatidylinositol (PI) mass remained unchanged. The total phospholipid content and the cholesterol/phospholipid ratio were essentially unaffected by 2OHOA treatment, despite the modest increase in cholesterol (20%) detected in treated cells. In addition, the analysis showed that SM levels increased in a time- and concentration-dependent manner (*SI Materials and Methods*).

We further analyzed the effect of 2OHOA on the phospholipid composition of human leukemia (Jurkat) cells, nonsmall lung cancer (A549) cells, additional human glioma cell lines (1321N1 and SF767) cells, and in nontumor (MRC-5) cells. Exposure to 2OHOA (200 μ M, 24 h) significantly increased the SM content of cancer cells (2.4-fold in Jurkat, 2.7-fold in A549, 2.2-fold in 1321N1, and 36.0% in SF767 cells) but not that of MRC-5 cells (Fig. 2A). These data not only revealed the ability of 2OHOA to regulate the phospholipid composition of tumor cells, but also they indicated that this effect was specific to cancer cells.

Table 1. Changes in phospholipid mass in control and treated cells

	Control		2OHOA	
	Mean	SD	Mean	SD
SM	42	4	193	16 ***
PC	249	16	176	13 ***
PS	70	3	40	5 ***
PI	36	2	31	6
PE	106	8	46	3 ***
Total PL	463	79	486	38
Cholesterol	172	16	205	10**
Cholesterol/PL	0.38	0.04	0.42	0.03

Phospholipid composition of U118 cells in the absence (control) or presence of 2OHOA (200 μ M, 72 h). Total lipid extracts were separated by TLC as described in *Materials and Methods*. Values are expressed as mass (nmol/mg protein) and represent mean \pm SEM; $n = 4-5$; PI, phosphatidylinositol; PL, phospholipids; PS, phosphatidylserine; *, $P < 0.05$; **, $P < 0.01$; ***, $P < 0.001$, Student's t test.

We used a number of analogues (200 μ M, 24 h) to investigate the structural bases underlying the regulatory effects of 2OHOA on SM focusing on the fatty acid length, the presence and number of double bonds, and the substitution at C-2 (Fig. 2B). The failure of oleic acid (18:1n-9) and 2-methyloleic acid (2Me-18:1n-9) to significantly affect SM levels indicated that the presence of the hydroxy group at C-2 is crucial. In addition, SM levels only increased when cells were treated with 18-C fatty acids containing at least one double bond. Therefore, SM accumulation induced by 2OHOA appears to be strictly related to the structure of the compounds.

Because of the rapid increase in SM, in addition to the decrease in PC content (Table 1), we assessed the SMS activity in the presence of 2OHOA. SMS activity was 3.6-fold higher than in untreated cells after 24 h of treatment (200 μ M) (Fig. 3A). Importantly, SMS activity increased 85% after 5 min of treatment, indicating that 2OHOA has an extremely rapid effect on SMS. To demonstrate that 2OHOA directly interacts with SMS, a cell postnuclear supernatant was incubated with NBD-C6-Cer (0.1 μ g/ μ L) and 2OHOA (200 μ M) for 2 h. In these *in vitro* conditions, 2OHOA increased SMS activity 80% (Fig. 3B), indicating a direct interaction between the drug and the enzyme.

To demonstrate the importance of SMS activation in 2OHOA's effects against tumors, we examined if SMS inhibition affected cell cycle progression. Thus, when A549 cells were exposed to 2OHOA (200 μ M, 16 h) in the presence of the SMS inhibitor D609 (350 μ M) (14, 15), the effect of 2OHOA on SM levels was reversed from 1.7-fold increase in the absence of D609 to 1.2-fold in its presence, indicating that 2OHOA was not able to exert its effect on SMS (Fig. 4A). Accordingly, the distribution of cells in the G_1 phase of the cell cycle shifted from $50 \pm 5.0\%$ in the absence of D609 to $40 \pm 4.1\%$ cells in its presence (values compared to control $31 \pm 1.4\%$; Fig. 4B), showing that SMS inhibition diminishes 2OHOA capability to induce cell cycle arrest.

The specific SM binding protein, lysenin (16), showed that the newly generated SM accumulated mainly at the plasma membrane (Fig. 5A). To understand the consequences that the dramatic changes in phospholipid composition provoked by 2OHOA on the structure and biophysical properties of the plasma membrane, we prepared model membranes with compositions mimicking the major alterations observed (Table 1). These membranes were labeled with one of two membrane probes: diphenylhexatriene (DPH), a fluorophore that shows no preference between the l_d (liquid disordered) and l_o (liquid ordered) phases, or t -PnA (*trans*-parinaric acid), which preferentially incorporates into l_o membrane domains (17).

The increase in DPH steady-state fluorescence anisotropy (DPH $\langle r \rangle$) in liposomes mimicking treated cells (Fig. 5B) was indicative of an increase in the general lipid order as this parameter reflects the global order of the acyl chains within the lipid bilayer membrane (9). Because the molar cholesterol fraction was

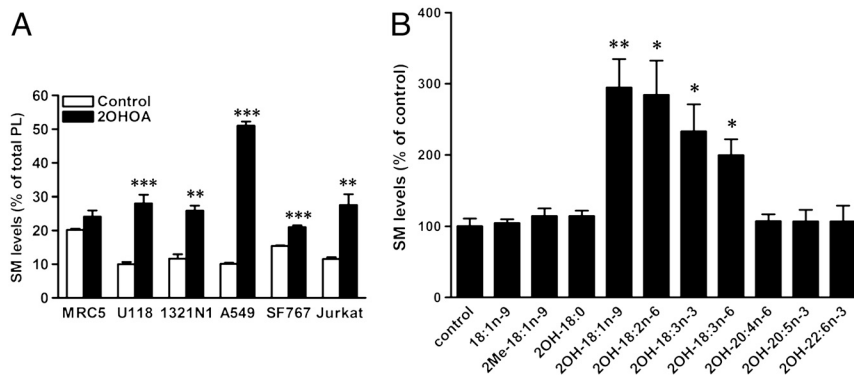


Fig. 2. The 2OHOA compound increases SM content in human tumor cells. Lipids were separated by thin-layer chromatography (TLC) and the phospholipid mass was determined by measuring the lipid phosphorus content of the different bands. (A) SM content in different cell lines (MRC-5, U118, Jurkat, SF767, and 1321N1 cells) after treatment with 2OHOA (24 h, 200 μ M). (B) SM content after treatment of U118 cells with different fatty acids (200 μ M, 24 h); 2Me-18:1n-9, 2-methyloleic acid; 2OH-20:4n-6, 2-hydroxyarachidonic acid; 2OH-22:6n-3, 2-hydroxydocosahexaenoic acid; 2OH-20:5n-3, 2-hydroxyeicosapentaenoic acid; 2OH-18:2n-6, 2-hydroxylinoleic acid; 2OH-18:3n-3, 2-hydroxy- α -linolenic acid; 2OH-18:3n-6, 2-hydroxy- γ -linolenic acid; 2OH-18:1n-9, 2-hydroxyoleic acid; 2OH-18:0, 2-hydroxystearic acid; 18:1n-9, oleic acid. Values represent the mean \pm SEM; $n = 3$; *, $P < 0.05$; **, $P < 0.01$; ***, $P < 0.001$.

similar in treated and control cells (Table 1), the increase in the lipid bilayer order was probably related to the marked increase in SM content. In addition, the changes in phospholipid composition induced an increase in the t -PnA long lifetime component (τ_{long}), indicating that the ordered domains became more ordered and more compact (Fig. 5C).

Discussion

From the molecular point of view, 2OHOA is a first-in-class anticancer lipid because its mechanism of action is not shared by other drugs used to treat cancer. However, its mechanism of action is yet to be fully elucidated, especially with respect to the first of the series of molecular events triggered by this molecule. In the present study, we show that 2OHOA activates SMS isozymes, inducing a rapid increase in the membrane levels of SM. In addition, this effect appears to be strongly associated with its structure, as only C-18 fatty acids with one or more double bonds and a hydroxyl moiety at C-2 induce SM accumulation.

Our aim was to investigate the effects of 2OHOA on the composition and structure of noncancer and cancer cell membranes, and the relationship of the changes induced with its activity against tumors. In the present work, we demonstrated that 2OHOA induces marked changes in the lipid composition of glioma cells by increasing SM mass in a time- and concentration-dependent manner (Table 1). Similar changes were observed in other glioma, leukemia, and lung cancer cell lines (Jurkat, 1321N1, SF767, and A549 cells), whereas no such differences in phospholipid composition were observed in nontumor MRC-5 cell membranes (Fig. 2A). The incapacity to produce relevant effects on nontumor MRC-5 cells could be due to the fact that

these cells already contain high levels of SM, such that SMS activation cannot further increase the amount of this lipid in membranes. Accordingly, lower SM levels in different human tumor tissues when compared to normal tissues (colon, breast, leukemic, esophagus, and brain) have been already described (18). Thus, the markedly lower levels of SM in cancer cells suggest that the malignant transformation of glioma and other cancer cells not only requires the activation of certain oncoproteins (e.g., Ras) but also, the modification of the membrane structure to permit their membrane docking and proliferative signal propagation (see below).

The 2OHOA compound augments both SMS1 and SMS2 activities, whereas it has no effect on SMS mRNA and protein levels. Interestingly, activation of SMS by 2OHOA turned out to be extremely rapid and sustained, probably due to the direct interaction between 2OHOA and SMS (Fig. 2A). This direct interaction is likely to explain the structural relationship between the fatty acid structure and SMS activation (Fig. 1B). Indeed, we found that (i) the 2-hydroxy moiety, (ii) 18 C atoms, and (iii) at least one double bond in the fatty acid structure were crucial to induce SM accumulation. An important question was the source of ceramides needed to sustain the large increase in SM. In this case, HPLC analysis showed that sphingosine mass increased 5.4-fold in cells exposed to 2OHOA (200 μ M, 48 h), suggesting the activation of at least the salvage pathway as sphingosine is only generated through this route (19).

In model membranes that mimic the lipid composition of U118 cell membranes before and after treatment with 2OHOA, a slight increase in the fraction of l_o domains, but a rather marked rise in the membrane hydrophobic core packing, was observed,

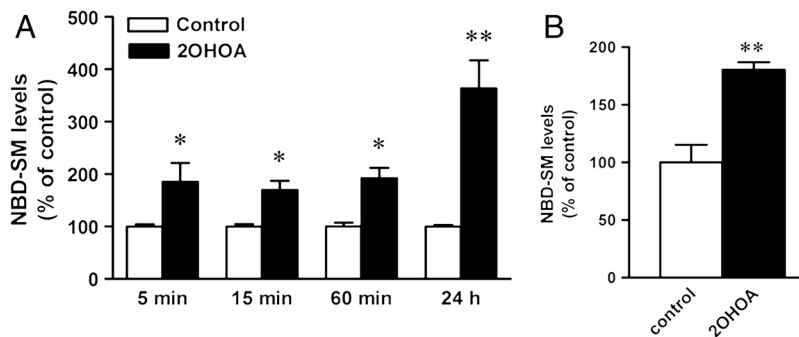


Fig. 3. Rapid and direct activation of SMS by 2OHOA in U118 cells. (A) Effect of the length of treatment on NBD-C6-SM levels. Cells were incubated with NBD-Cer (4 h, 3 μ M) and treated with 2OHOA (200 μ M) for different times. (B) In vitro SMS activity assay (see *Materials and Methods*). Values represent the mean \pm SEM; $n = 3$; *, $P < 0.05$; **, $P < 0.01$.

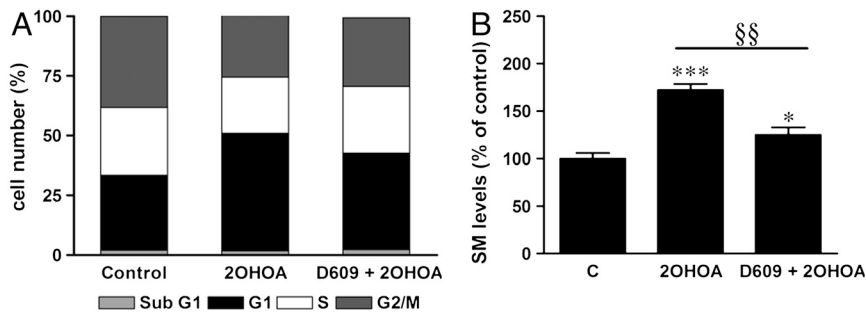


Fig. 4. Inhibition of SMS by D609 diminishes the effect of 2OHOA on cell cycle progression. (A) Effect of SMS inhibition on cell cycle progression. Bar graphs show the percentage of A549 cells in Sub G₁, G₁, S, and G₂/M phases with respect to the total cell number. (C) Effect of SMS inhibition on SM content. Values represent the mean \pm SEM; $n = 3$; *, $P < 0.05$; **, $P < 0.01$; ***, $P < 0.001$. In this case, § indicates a significant effect of the inhibition as compared with the treatment (§§, $P < 0.01$).

probably associated with an increase in the size of the l_o domains (10). The enhancement in global membrane order was associated to the substantial increase in SM content, as the amount of cholesterol was only modestly modified. Therefore, the alterations in phospholipid composition observed in treated cells modify the biophysical properties of the cell membrane, particularly the packing of SM/cholesterol-enriched l_o domains. This change in the structure of membrane microdomains alters the interaction of relevant peripheral signaling proteins with the membrane and the subsequent propagation of messages into the cell.

In this context, two different molecular mechanisms are known to be activated by 2OHOA in cancer cells that may be triggered by increases in membrane SM. Thus, in leukemia cells, 2OHOA induces Fas receptor (FasR) capping favoring spontaneous interactions of FasR subunits and the activation of the extrinsic apoptosis pathway (4). Moreover, FasR capping has been linked to SM synthesis (20), such that the changes in the composition and structure of membranes induced by 2OHOA also explain the induction of apoptosis observed in Jurkat cells (4).

On the other hand, 2OHOA may induce translocation of Ras and cell cycle arrest in human glioma and lung cancer cells. Ras has a bulky isoprenyl lipid anchor and requires l_d microdomains with loose surface packing (as PE-rich domains) to permit its insertion into the membrane, which is necessary for subsequent interactions of Ras with upstream (e.g., EGFR) and downstream

(e.g., Raf) proteins in the MAPK pathway. Therefore, the increase in SM diminishes the l_d domains and augments the l_o regions, the net result being an inactivation of the MAPK pathway. Through cross-talk, the inhibition of this pathway can impair the PI3K/Akt pathway and consequently the cell cycle machinery (cyclin/cdk complexes). In addition, increases in 1,2-DAG could be involved in the relatively sustained and mild activation of PKC (about 3-fold) (3). This activation could lead to the overexpression of the CDK inhibitors, p21^{Cip1} and p27^{Kip1}, which are associated with the hypophosphorylation of the retinoblastoma protein and the ensuing inhibition of E2F-1 and β -catenin (2, 3). The cellular outcome of these molecular processes is the inhibition of cell growth, and the induction of cell differentiation and autophagy (1, 21, 22).

Some studies show that SMS inhibition and the ensuing ceramide accumulation are associated with cell cycle arrest (23) or cell death (24, 25) However, reduced SM synthesis causes resistance to certain apoptosis inducing drugs (26, 27). In addition, increased SM membrane content enhanced Fas- and TNF- α -induced apoptosis through an efficient clustering of FasR or by increasing TNF- α receptor exposure at the plasma membrane (20, 26). Analogously, decreased SM levels protected THP-1 derived macrophages from lipopolysaccharide-induced apoptosis, an effect linked to a decrease in cell surface TLR-4 expression (26). For all these reasons, the physiological significance of

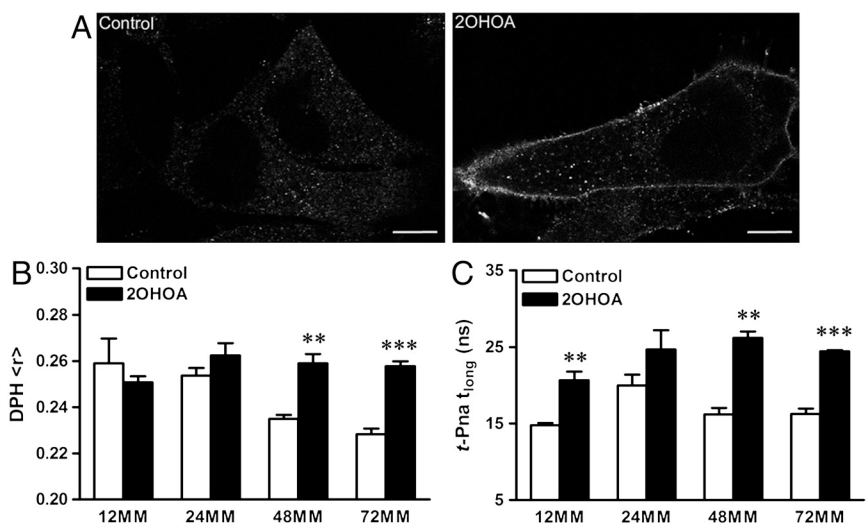


Fig. 5. Changes in phospholipid composition induced by 2OHOA increase the global order of model membranes. (A) Representative confocal sections of U118 cells labeled with lysenin showing increased SM plasma membrane levels after 2OHOA treatment (200 μ M, 72 h). Cells were fixed and incubated with lysenin as described in *Materials and Methods*. Scale bar, 10 μ m. (B) The 2OHOA compound induces an increase in the global order of the membrane. Steady-state fluorescence anisotropy, $\langle r \rangle$, of DPH in PC:PE:SM:Cholesterol mixtures at 24 $^{\circ}$ C. (C) Treatment induces an increased packing of the l_o domains. Long lifetime component of the mean fluorescent lifetime, τ_{long} , of t-Pna in POPC:POPE:PSM:Cholesterol mixtures at 24 $^{\circ}$ C. MM, model membrane. Values represent the mean of triplicates \pm SD; $n = 3$; **, $P < 0.01$; ***, $P < 0.001$.

SMS may go beyond the mere formation of SM acting as a regulator of ceramide levels, but, in turn, SM seems to modulate the cell surface expression of receptors by modifying lipid raft properties (28). In this context, our results demonstrated the important role that SMS activation plays in 2OHOA antitumor mechanism attributing proapoptotic properties to the large and sustained SMS activation. In any case, the controversial results clearly point to a complex scenario, where the effect of SMS activation on cell fate would depend on, among other factors, the cell line, the type and intensity of the stimuli (28), and even on the specific pool of regulated ceramides (33).

In summary, we show that the cancer cell lines investigated had markedly and significantly lower levels of SM than noncancer (MRC-5) cells, which suggests that remodeling of the plasma membrane composition and structure is a relevant aspect of the malignant transformation that generates the cancerous phenotype. Furthermore, we demonstrate that SMS activation by 2OHOA could be the first and critical event in its effects against tumors. Because 2OHOA is a potent and specific lipid to combat tumors, with no side effects at therapeutic doses, the data presented not only introduce the known activator of SMS, but also they define a molecular target for the design of new compounds against cancer.

Materials and Methods

Cell Culture. Human glioma (U118, 1321N1, SF767), human nonsmall lung adenocarcinoma (A549), Jurkat-T lymphoblastic leukemia cells, and MRC5 human fibroblast cells were obtained from the American Type Culture Collection. The cells were maintained as described previously (1).

Lipids. The 2OHOA compound (Good Manufacturing Practice quality) was obtained from Avanti Polar Lipids, and its purity was assessed as described previously (1). The 2OH-18:0 and 2Me-18:1n-9 were kindly provided by Oliver Vögler (Department of Biology, University of the Balearic Islands, Palma, Spain). The rest of the 2-hydroxy fatty acids were synthesized by Medalchemy SL. The 1-palmitoyl-2-oleoyl-*sn*-glycero-3-phosphocholine (POPC), N-palmitoyl-sphingomyelin (PSM), and 1-palmitoyl-2-oleoyl-*sn*-glycero-3-phosphoethanolamine (POPE) were purchased from Avanti Polar Lipids. Oleic acid was purchased from Sigma Chemicals Company. NBD-C6-Cer and the *t*-PnA and DPH probes were purchased from Invitrogen, Molecular Probes. LUDOX (diluted 50 wt % colloidal silica in water) and cholesterol were from Sigma-Aldrich. All solvents and probe solutions used were spectroscopic-grade purity (Merck).

Lipid Analysis. The cellular lipids were extracted directly from the frozen monolayer of cells by a modified *n*-hexane:2-propanol (3:2, vol/vol) extraction (29, 30). Protein levels were measured using the bicinchoninic assay according to the manufacturer's instructions (Thermo Scientific). Individual phospholipid classes and neutral lipids were separated by TLC or by high-performance TLC (HPTLC) on Whatman silica gel-60 plates (20 × 20 cm or 10 × 10 cm) using chloroform/methanol/acetic acid/water (55:37.5:3:2 by volume). For TLC, the phospholipid mass was determined by assaying the lipid phosphorus (31), whereas for HPTLC separation, plates were air-dried, sprayed with 8% (wt/vol) H₃PO₄ containing 10% (wt/vol) CuSO₄, and charred at 180 °C for 10 min; then, lipids were quantified by photodensitometry. The lipid fractions were identified using authentic standards (Larodan).

SMS Activity Assay in Cell Culture. [Adapted from Tafesse, et al. (23).] Briefly, U118 cells were incubated for 4 h with NDB-C6-Cer (3 μM). NBD-C6-phospholipids were separated by HPTLC and were visualized on a Bio-Rad Molecular Imager FX and quantified using Quantity One software (Bio-Rad).

In Vitro SMS Activity Assay. [Adapted from Villani et al. (26) and Ding et al. (32).] U118 cells were homogenized in ice-cold lysis buffer (50 mM Tris/HCl, 1 mM EDTA, 1 mM PMSF, 8% CHAPS (wt/vol), pH 7.4) by passing 20 times through a 28 gauge needle. The cell lysate was centrifuged at 500 × *g* for 5 min at 4 °C, and the enzymatic activity was measured in the postnuclear supernatant (100 μg of protein). The substrate was a mixture of 0.1 μg/μL of NBD-C6-Cer, 0.01 μg/μL of synthetic PC and PE resuspended by sonication and vortexing until it was clear in 50 mM Tris/HCl, 25 mM KCl and 1 mM EDTA, pH 7.4. The substrate was diluted 1:1 with the proteins resuspended in reaction buffer. The reaction was stopped on ice by addition of 2 vol of chloroform/methanol (1:2, vol/vol) after the incubation period (2 h in dark).

Inhibition Experiments. A549 cells were incubated with D609 for 16 h (350 μM, a gift from A. Llebaria, Department of Biomedical Chemistry, Institut d'Investigacions Químicas i Ambientals de Barcelona-Centro Superior de Investigaciones Científicas, Barcelona, Spain), and 2OHOA (200 μM) was added 1 h after the addition of D609. The effect on the cell cycle was evaluated by flow cytometry. After trypsinization, A549 cells were fixed with ice-cold 70% ethanol for 1 h at 4 °C, centrifuged for 5 min at 1,260 × *g*, and resuspended in a sodium citrate (38 mM, pH 7.4). Then, cells were incubated for 20 min at 37 °C with buffer A [sodium citrate (38 mM, pH 7.4), 50 μg/mL propidium iodide, and 5 μg/mL RNase A (Sigma-Aldrich)] and analyzed on a Beckman Coulter Epics XL flow cytometer. Cell populations in the different phases of cell cycle (subG₁, G₀/G₁, S, and G₂/M) were determined on the basis of their DNA content.

Immunofluorescent Labeling of SM by Lyсенin. Cells were grown on Chambered Coverglass (Lab-Tek™ II, Thermo Fisher Scientific Inc.) in the presence or absence of 2OHOA (200 μM, 72 h). SM was labeled with lysenin as described previously (16) with minor modifications (see *SI Materials and Methods*). Images were acquired on a Leica TCS SP2 spectral confocal microscope at 630× optical magnification and 3× digital magnification. The images were analyzed with the software provided by the manufacturer.

Liposome Preparation and Fluorescence Measurements. Multilamellar vesicles (MLV) of POPC, POPE, PSM, and cholesterol mixtures were prepared with either *t*-PnA or DPH, or with no probe. MLV suspensions were prepared as previously (10) (molar proportions of each lipid is given in *SI Materials and Methods*). The probe:lipid ratios used were 1:200 for DPH and 1:500 for *t*-PnA. Fluorescence measurements were obtained with a Horiba Jobin Yvon FL-1057 Tau 3 spectrofluorometer, carrying out the experiments at 24 °C.

Statistics. Statistical analysis was performed using GraphPad Prism 4.01 (GraphPad Software Inc.). Unless specified, the data are expressed as the mean ± SEM, at least three independent experiments, the value represented by *n*. The statistical significance of the mean difference was determined by Student's *t* test. The asterisks indicate a significant effect of the treatment when compared with the control: *, *P* < 0.05; **, *P* < 0.01; ***, *P* < 0.001.

ACKNOWLEDGMENTS. We thank Dr. E. J. Murphy, Dr. D. H. Lopez, and Dr. X. Busquets for their comments during this study and the elaboration of the manuscript. We thank Dr. S. Rodriguez-Cuenca for his invaluable technical support with the real time RT-PCR and siRNA experiments. This work was supported by the Ministerio de Ciencia e Innovación Grants BIO2010-21132 and IPT-010000-2010-016, by the Marathon Foundation, and by the Fundação para a Ciência e Tecnologia Grant PEst-OE/QUI/UI0612/2011. G.B.-C. holds a "Juan de la Cierva" contract from the Ministerio de Ciencia e Innovación; M.L.M. and M.A.N.-S. hold fellowships from the Conselleria d'Economia, Hisenda i Innovació, Govern Balear; F.G.-S. holds a contract from the "Fundación Científica de la Asociación Española Contra el Cáncer"; A.M.-E. holds a MCINN fellowship.

- Lladó V, et al. (2009) Pivotal role of dihydrofolate reductase knockdown in the anticancer activity of 2-hydroxyoleic acid. *Proc Natl Acad Sci USA* 106:13754–13758.
- Martínez J, et al. (2005) The repression of E2F-1 is critical for the activity of Minerval against cancer. *J Pharmacol Exp Ther* 315:466–474.
- Martínez J, et al. (2005) Membrane structure modulation, protein kinase C alpha activation, and anticancer activity of minerval. *Mol Pharmacol* 67:531–540.
- Lladó V, et al. (2010) Minerval induces apoptosis in Jurkat and other cancer cells. *J Cell Mol Med* 14:659–670.
- Escribá PV, Sastre M, García-Sevilla JA (1995) Disruption of cellular signaling pathways by daunomycin through destabilization of nonlamellar membrane structures. *Proc Natl Acad Sci USA* 92:7595–7599.

- Barceló F, et al. (2004) The hypotensive drug 2-hydroxyoleic acid modifies the structural properties of model membranes. *Mol Membr Biol* 21:261–268.
- Gajate C, Mollinedo F (2007) Edelfosine and perifosine induce selective apoptosis in multiple myeloma by recruitment of death receptors and downstream signaling molecules into lipid rafts. *Blood* 109:711–719.
- Simons K, Toomre D (2000) Lipid rafts and signal transduction. *Nat Rev Mol Cell Biol* 1:31–39.
- de Almeida RF, Fedorov A, Prieto M (2003) Sphingomyelin/phosphatidylcholine/cholesterol phase diagram: Boundaries and composition of lipid rafts. *Biophys J* 85:2406–2416.

Supporting Information

Barceló-Coblijn et al. 10.1073/pnas.1115484108

SI Materials and Methods

Cell Viability Assay. Viability was evaluated by measuring the mitochondrial dehydrogenase activity of living cells using the XTT method (2,3-bis[2-methoxy-4-nitro-5-sulfophenyl]-2H-tetrazolium-5-carboxyanilide inner salt) according to the manufacturer's instructions. Briefly, cells were seeded in flat-bottom 96-well plates ($2 \cdot 10^4$ cells per mL, 200 μ L per well) at 37 °C for the times indicated, and XTT (0.2 mg/mL in RPMI medium 1640 without phenol red; Sigma-Aldrich) was added during the last 8 h. The absorbance of the resulting solution was measured at 450 nm. The absorbance at 690 nm was also measured as a background measurement and subtracted from the 450-nm value.

Cell Surface Sphingomyelin Synthase (SMS) Activity Assay. The cell surface SMS activity assay was adapted from Tafesse et al. (1). Briefly, subconfluent U118 cells were exposed to 2-hydroxyoleic acid (2OHOA) (200 μ M) for 6 h, washed with ice-cold HBSS, and then incubated for 3 h at 0 °C in HBSS containing 3 μ M NBD-C6-Cer and 1% (wt/vol) fatty acid-free BSA and 2OHOA (200 μ M). After a 30-min incubation in HBSS +1% BSA (wt/vol), the medium was collected, and the lipids from the medium and the cells were extracted and analyzed (2).

Immunofluorescent Labeling of Sphingomyelin (SM) by Lysenin. Cells were grown on Chambered Coverglass (Lab-Tek™ II, Thermo Fisher Scientific Inc.) in the presence or absence of 2OHOA (200 μ M, 72 h) as indicated above. SM was labeled with lysenin as described previously (3) with minor modifications, carrying out all steps at room temperature. After washing twice for 5 min with phosphate buffer 0.1 M (PB: NaH₂PO₄ 20 mM, Na₂HPO₄ 80 mM, pH 7.4), the cells were fixed with 4% paraformaldehyde in PB for 20 min and washed again with PB. To quench any excess of the reactive paraformaldehyde groups, the cells were incubated with 0.1 M NH₄Cl in PB for 15 min and washed again twice with PB. After blocking with 2% BSA in PB for 30 min, the cells were incubated with lysenin (1 μ g/mL in blocking solution; PeptaNova GmbH) for 2 h and washed twice with PB for 5 min. After incubation for 1 h with a rabbit antilysenin antiserum (1:500 in blocking solution; PeptaNova GmbH), the antiserum was detected by incubating for 1 h with a fluorescent secondary antibody (Alexa Fluor 488 conjugated goat antirabbit antibody diluted 1:200; Molecular Probes; excitation at 488 nm and detection at 510–550 nm). After washing the cells twice with PB for 5 min, images were acquired on a Leica TCS SP2 spectral confocal microscope at 630 \times optical magnification and 3 \times digital magnification (approximately 1,800 \times total magnification), and the images were analyzed with the software provided by the manufacturer.

Lipid Extraction and Measurement of Sphingosine and Sphingosine-1-Phosphate (S1P). Lipids were extracted by a modified two-step lipid extraction described previously (4). Accordingly, 100 μ L of the sample was transferred into a siliconized glass tube and 200 pmol of dihydro-S1P was added as an internal standard. After alkalization with 100 μ L of a 3 N NaOH solution, the lipids were extracted in 1 mL chloroform and 1 mL 1 N NaCl. After centrifugation (300 \times g, 5 min) the organic phase was reextracted with 0.5 mL methanol, 0.5 mL 1N NaCl, and 50 μ L 3N NaOH. The collected aqueous phases were acidified with 100 μ L concentrated HCl and extracted twice with 1.5 mL chloroform. The combined organic phases were then evaporated and dried lipids resolved in 325 μ L methanol/0.07 M K₂HPO₄ (8:2) by rigorous vortexing and sonicating on ice for 5 min. A derivatization mix-

ture of o-phthaldialdehyde, mercaptoethanol, ethanol, and boric acid solution (pH 10.5) was prepared and added to the lipid fractions (resolved in methanol/0.07 M K₂HPO₄) for 15 min at room temperature. The derivatives were analyzed on a Merck Hitachi LaChrom HPLC system (Merck Hitachi). Fluorescence was measured at $\lambda_{em} = 455$ nm after separation at 35 °C on an RP 18 Kromasil column (Chromatographie Service). The flow rate was adjusted to 1.3 mL/min and a gradient of methanol and 0.07 M K₂HPO₄ was used. The resulting profiles were evaluated using the Merck system manager software.

Electrophoresis (SDS/PAGE), Immunoblotting, and Protein Quantification. Cells were incubated in six-well culture plates in the presence or absence of 2OHOA, under the experimental conditions indicated above. The cells were then washed twice with PBS and harvested with a Teflon cell scraper in 300 μ L 10 mM Tris-HCl buffer containing 50 mM NaCl, 1 mM MgCl₂, 2 mM EDTA, 1% SDS, 5 mM iodoacetamide, 1 mM phenylmethylsulfonylfluoride, 1 μ M sodium orthovanadate, and 1 μ M cantharidin, pH 7.4. The cells were homogenized by ultrasound (3 times 10-s cycles at 50 W) in a Braun Labsonic U sonicator (10% cycle), and 30 μ L aliquots were removed for total protein quantification by the Bradford method (BioRad). For immunoblotting, 25 μ g of total protein was resolved on the same SDS-polyacrylamide gel (9% polyacrylamide) and transferred to nitrocellulose membranes (Whatman, Schleicher and Schuell). For SMS1, SMS2, DHFR, and α -tubulin membranes were incubated with blocking solution (PBS containing 5% nonfat dry milk) for 1 h at room temperature and then overnight at 4 °C in fresh blocking solution containing the specific primary antibodies: rabbit anti-SMS1 (1:1,000; Santa Cruz); mouse anti-SMS2 (1:1,000; Abcam); mouse antiDHFR (1:250; Abcam); mouse anti- α -tubulin (1:10,000; Sigma). The membranes were then incubated for 60 min in the dark with a fluorescent-labeled secondary antibody (1:5,000; Casa Commercial) with 3% BSA in PBS, and then the proteins were visualized and quantified by the Odyssey Infrared Imaging System (LI-COR, Inc.). The protein content measured for a given protein was normalized to the α -tubulin content.

Quantitative Reverse Transcription–Polymerase Chain Reaction (QRT-PCR). QRT-PCR was used to determine the regulatory effects of 2OHOA on the levels of SMS1 and SMS2 mRNA. Accordingly, cells were incubated in the presence or absence of 2OHOA for 24 h and the total RNA was then extracted from U118 cells using the RNeasy Mini kit in combination with the RNase-free DNase kit (Qiagen) according to the manufacturer's instructions. Reverse transcription of 1 μ g of DNA was carried out using the Transcriptor First Strand cDNA Synthesis Kit (Roche Diagnostics) according to the manufacturer's instructions, and the cDNA samples obtained were stored at –20 °C. For PCR amplification, the primers designed were based on the SMS1 and SMS2 sequences in GenBank: 5'-GAG CCT CTG GAG CAT TTC AC-3' (SMS1 forward), 5'-TGC TCC ATT TTC AGG GTT TC-3' (SMS1 reverse), 5'-CAA CAC TGT TTT GGT GG-3' (SMS2 forward), and 5'-GGA GAA GCA GCA AGG AAT TG-3' (SMS2 reverse). As endogenous control, the expression of β -actin was determined using the following primers: 5'-GCG GGA AATCGT GCG TGA CAT T -3' (forward primer) and 5'-CTA CCT CAACTT CCA TCA AAG CAC -3' (reverse primer). Real-time PCR amplifications were carried out in a StepOne Plus thermal cycler (Applied Biosystems) using the SYBR Premix Ex Taq 2X (Perfect Real-Time, Takara). The cDNAs were initially denatured for 30 s at

95 °C prior to thermal cycling. DNA amplification and fluorescence quantification was determined over 35 cycles with a 5-s denaturation step at 95 °C, followed by a 34-s annealing/extension step at 60 °C. Fluorescence detection and quantification was carried out after each DNA extension step, and the data were analyzed using the StepOne software (version 2.0). The ratio between the expression of SMS1 or SMS2 and β -actin (whose expression is not modulated by 2OHOA) was determined by means of the equation described by Pfaffl (5). This value was used to calculate the relative expression in 2OHOA-treated cells with respect to untreated cells (control = 1). Melting curve analysis and agarose gel electrophoresis were used to further characterize the PCR products.

Liposome Preparation. Lipid stock solutions were prepared in chloroform, except for 1-palmitoyl-2-oleoyl-sn-glycero-3-phosphoethanolamine (POPE) that was dissolved in chloroform:methanol (2:1, vol/vol). Multilamellar vesicles (MLV) of quaternary 1-palmitoyl-2-oleoyl-sn-glycero-3-phosphocholine (POPC), POPE, N-palmitoyl-sphingomyelin (PSM), and cholesterol mixtures were prepared with either *t*-PnA or diphenylhexatriene (DPH), or with no probe (blank). MLV suspensions were prepared as previously (6), and the molar proportions of each lipid is given in Table S1. Total lipid concentration in the MLV suspensions was 0.2 mM in every sample, and the medium used for suspension was sodium phosphate 10 mM, NaCl 150 mM, EDTA 0.1 mM buffer, pH 7.4. The probe:lipid ratios used were 1:200 for DPH and 1:500 for *t*-PnA. The lipid concentrations for phospholipids were determined according to the phosphorous content and by weight for all lipids. Probe concentration in stock solutions were determined by absorption spectrophotometry carried out with a Jasco V-560 UV/Vis spectrophotometer as described previously (6).

Fluorescence Measurements and Data Analysis. Fluorescence measurements were obtained with a Horiba Jobin Yvon FL-1057 Tau

3 spectrofluorometer, carrying out the experiments at 24 °C. All the results are the mean \pm SD of three independent samples.

For steady-state measurements (450 W Xe arc lamp light source), the samples were under constant magnetic stirring, and the excitation/emission wavelengths were 358 nm/430 nm for DPH or 303 nm/404 nm for *t*-PnA. The steady-state anisotropy ($\langle r \rangle$) was calculated according to the following equation:

$$\langle r \rangle = (I_{VV} - G \times I_{VH}) / (I_{VV} + 2G \times I_{VH}), \quad [S1]$$

in which G is the instrumental correction factor. “V” and “H” represent the vertical and horizontal orientations of the polarizers, and the order of the subscripts corresponds to excitation and emission. An adequate blank was subtracted from each intensity reading.

For the time-resolved measurements obtained by the single photon counting technique, nanoLED N-320 (Horiba Jobin Yvon) was used for the excitation of *t*-PnA and the emission wavelength was 404 nm. Diluted LUDOX was used as the scatterer to obtain the instrumental response function. The TRFA Data Processor version 1.4 program (Scientific Software Technologies Center) was used to analyze the experimental fluorescence decays, and an adequate blank decay was acquired and subtracted from the respective samples. The decays were analyzed by fitting a sum of exponentials,

$$I(t) = \sum_{i=1}^n \alpha_i \exp(-t/\tau_i), \quad [S2]$$

where α_i and τ_i are the normalized amplitude and lifetime of the component i , respectively. The long lifetime component (τ_{long}) of this probe is specifically due to the ordered domains, and directly reflects their composition and acyl chain packing (7).

1. Tafesse FG, et al. (2007) Both sphingomyelin synthases SMS1 and SMS2 are required for sphingomyelin homeostasis and growth in human HeLa cells. *J Biol Chem* 282:17537–17547.
2. Bligh EG, Dyer WJ (1959) A rapid method of total lipid extraction and purification. *Can J Biochem Physiol* 37:911–917.
3. Yamaji A, et al. (1998) Lysenin, a novel sphingomyelin-specific binding protein. *J Biol Chem* 273:5300–5306.
4. Prakash H, et al. (2010) Sphingosine kinase-1 (SphK-1) regulates Mycobacterium smegmatis infection in macrophages. *PLoS One* 5:e10657.
5. Pfaffl MW (2001) A new mathematical model for relative quantification in real-time RT-PCR. *Nucleic Acids Res* 29:e45.
6. de Almeida RF, Loura LM, Fedorov A, Prieto M (2005) Lipid rafts have different sizes depending on membrane composition: A time-resolved fluorescence resonance energy transfer study. *J Mol Biol* 346:1109–1120.
7. Aresta-Branco F, et al. (2011) Gel domains in the plasma membrane of *Saccharomyces cerevisiae*: Highly ordered, ergosterol-free, and sphingolipid-enriched lipid rafts. *J Biol Chem* 286:5043–5054.

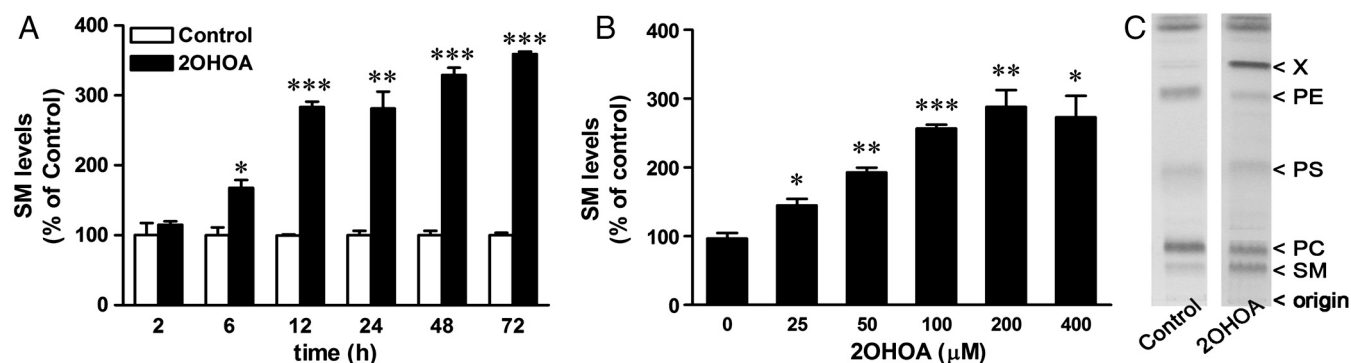


Fig. S1. The 2OHOA compound increases SM content in a time- and concentration-dependent manner in U118 human glioma cells. (A) SM content after treatment with 2OHOA (200 μ M) for different times in U118 cells. (B) SM content after treatment of U118 cells with different concentrations of 2OHOA (24 h). (C) Representative TLC analysis of the total lipids extracted from control and treated (72 h, 200 μ M) U118 cells. In all cases, SM levels were determined by HPTLC and expressed as the percentage with respect to the untreated cells. Values represent the mean \pm SEM, $n = 3$. *, $P < 0.05$, Student's t test; **, $P < 0.01$, Student's t test; ***, $P < 0.001$, Student's t test comparing control.

